



Structural characterization and electrochemical properties of novel salicylidene phosphonate derivatives

Mustafa Dolaz^{a,*}, Vickie McKee^b, Muhammet Köse^b, Ayşegül Gölçü^c, Mehmet Tümer^c

^a Kahramanmaraş Sutcu Imam University, Faculty of Engineering and Architecture, Department of Environmental Engineering, K.Maras, Turkey

^b Univ Loughborough, Dept Chem, Loughborough LE11 3TU, Leics, England, United Kingdom

^c Kahramanmaraş Sutcu Imam University, Chemistry Department, 46100, K.Maras, Turkey

ARTICLE INFO

Article history:

Received 25 November 2009

Received in revised form 5 May 2010

Accepted 15 May 2010

Keywords:

Salicylidene
Phosphonate
Schiff base
X-ray
Electrochemical

ABSTRACT

In this study, three novel salicylidene phosphonate ligands, diethyl (4-((1*E*)-(2-hydroxyphenyl)methylidene)amino)benzyl)phosphonate (HL¹), diethyl (4-((1*E*)-(2-hydroxy-3-methoxyphenyl)methylidene)amino)benzyl)phosphonate (HL²) and diethyl (4-((1*E*)-(2,4-dihydroxyphenyl)methylidene)amino)benzyl)phosphonate (HL³) were synthesized and characterized by the analytical and spectroscopic techniques. We obtained their single crystals from the ethanolic solution. There are intramolecular phenol-imine hydrogen bonds in all three compounds between O1 and N1 atoms. The ligand HL³ contains a second phenol group and this is makes an intermolecular hydrogen bond with the phosphine oxide of a neighbouring molecule O2–O3 (under symmetry operation $-x, 0.5 + y, 0.5 - z$). In order to investigate the redox behaviours of the salicylidene phosphonate ligands (HL¹–HL³), we were studied electrochemical properties of the ligands at the different pH and scan rates.

© 2010 Elsevier B.V. All rights reserved.

1. Introduction

The Schiff bases, formed by the condensation of an amine with an aldehyde [1], usually coordinate to a metal through the imine nitrogen and another group, usually oxygen, nitrogen or sulfur situated on the original aldehyde. Condensation of the carbonyl function of a β -ketone with only one end of a diamine produces terdentate ligand and this can be make to undergo further condensation with another carbonyl function to produce unsymmetrical tetradentate Schiff base ligands. The Schiff bases are very important tools for the inorganic chemists as these are widely used to design molecular ferromagnets, in catalysis, in biological modeling applications, as liquid crystals and as heterogeneous catalysts [2]. Schiff base complexes are once again topical in connection with self-assembling cluster complexes [3].

The transition metal complexes having oxygen and nitrogen donor Schiff bases possess unusual configuration, structural lability and are sensitive to molecular environment [4]. The environment around the metal center 'as coordination geometry, number of coordinated ligands and their donor group' is the key factor for metalloprotein to carry out a specific physiological function [5]. About 20 Zinc enzymes are known in which Zinc is generally tetrahedrally four coordinate and bonded to hard donor atoms such as nitrogen or oxygen [6]. Manganese plays an important role

in several biological redox-active system [7], a number of copper proteins including enzymes have been reported and proteins containing iron participate in oxygen transport [8]. The preparation of model complexes having similar spectroscopic features is perhaps the most important step to understand the structure and behaviour of these biological systems. Schiff base metal complexes attract considerable interest and occupy an important role in the development of the chemistry of chelate systems [9,10] due to the fact that especially these with N₂O₂ tetradentate ligands, such systems closely resemble metallo-proteins. Survey of the literature reveals an excellent work devoted to synthesis and characterization of many metal complexes of Schiff base [11,12], furthermore the coordination compounds of phosphonic acid and their esters with transition metal ions have been the subject of several studies due to the fact that complexes of such compounds exhibit biological activity [13].

In this study, we report synthesis and structural characterization of three novel salicylidene phosphonate ligands (HL¹–HL³). In addition, we also investigated the spectroscopic and electrochemical properties of the ligands.

2. Experimental

2.1. General

Salicylaldehyde, 3-methoxy-2-hydroxybenzaldehyde, 2,4-dihydroxybenzaldehyde, diethyl (4-aminobenzyl)phosphonate (starting material), and organic solvents were obtained from Fluka

* Corresponding author. Tel.: +90 344 2191460; fax: +90 344 2191052.

E-mail address: mdolaz@ksu.edu.tr (M. Dolaz).

and used as received, unless noted otherwise. Elemental analyses (C, H, N) were performed using a LECO CHNS 932 elemental analyzer. IR spectrum was obtained using KBr discs (4000–400 cm^{-1}) on a Shimadzu 8300 FT-IR spectrophotometer. The electronic spectra in the 200–500 nm range were obtained on a Perkin-Elmer Lambda 45 spectrophotometer. Molar conductance measurement of the Schiff base ligand (L) was determined in methanol ($\sim 10^{-3}$ M) at room temperature using a Jenway Model 4070 conductivity meter. Mass spectrum of the ligand was recorded on an LC/MS APCI AGILENT 1100 MSD spectrophotometer. ^1H NMR spectra of the ligands were recorded on Bruker – 300 instrument. TMS was used as internal standard and CDCl_3 as solvent.

The voltammetric measurements at a glassy carbon electrode was performed using a BAS 100 W (Bioanalytical System, USA) electrochemical analyzer. A glassy carbon working electrode (BAS; Φ : 3 mm diameter), an Ag/AgCl reference electrode (BAS; 3 M KCl) and platinum wire counter electrode and a standard one-compartment three-electrode cell of 10 mL capacity were used in all experiments. The glassy carbon electrode was polished manually with aqueous slurry of alumina powder (Φ : 0.01 μm) on a damp smooth polishing cloth (BAS velvet polishing pad), before each measurement. All measurements were realized at room temperature.

The pH was measured using a pH meter Model 538 (WTW, Austria) using a combined electrode (glass electrode–reference electrode) with an accuracy of ± 0.05 pH.

2.2. Preparation of the novel salicylidene phosphonate ligands (HL^1 – HL^3)

The salicylidene phosphonate ligands were prepared according to the similar methods. A solution of diethyl (4-aminobenzyl)phosphonate (0.243 g, 1 mmol) in ethanol (15 ml) was added drop wise to an ethanolic solution (30 ml) of the benzaldehyde derivatives (0.122 g for salicylaldehyde; 0.152 g for 3-methoxy-2-hydroxybenzaldehyde and 0.138 g for 2,4-dihydroxybenzaldehyde, 1 mmol) with stirring. The yellow solution was stirred and refluxed for 1 h and the solvent was evaporated in air. The yellow solid was separated by filtration through G4 sintered bed and washed thoroughly with hexane and water. Finally, the isolated compound was dried in vacuo over P_4O_{10} . Single crystals of the ligands (HL^1 – HL^3) were obtained by recrystallization from $\text{C}_2\text{H}_5\text{OH}$ solution.

HL^1 – Yield: 72%, m.p. 95 °C. color: yellow. Analysis Calc. for $\text{C}_{18}\text{H}_{22}\text{NO}_4\text{P}$: C, 62.24; H, 6.38; N, 4.03%. Found: C, 62.30; H, 6.35; N, 4.02%. Mass spectrum (LC/MS APCI): m/z 303 [$\text{M}+\text{H}-\text{OCH}_2\text{CH}_3$] $^+$. ^1H NMR: (CDCl_3 as solvent, δ in ppm): 1.26 (3H, t, $-\text{CH}_3$), 3.15 (2H, d, $-\text{P}-\text{CH}_2-$), 4.01 (2H, m, $-\text{CH}_2-$), 6.93–7.42 (8H, m, aromatic protons), 8.64 (1H, s, $-\text{CH}=\text{N}-$), 13.27 (H, s, $-\text{OH}$). UV-vis: (λ_{max} , nm; ϵ_{max} , $\text{M}^{-1}\text{cm}^{-1}$), CH_3OH as solvent: 380 (2.5×10^{-3}), 315 (7.1×10^{-3}), 294 (5.5×10^{-3}), 278 (1.0×10^{-4}), 245 (6.2×10^{-4}), 228 (8.8×10^{-4}). Infrared spectrum (cm^{-1} , KBr disk): 2960, 2845 $\nu(\text{CH}_2)$, 1625 $\nu(\text{C}=\text{N})$, 1245 $\nu(\text{P}=\text{O})$.

HL^2 – Yield: 84%, m.p. 115 °C. color: light yellow. Analysis Calc. for $\text{C}_{19}\text{H}_{24}\text{NO}_5\text{P}$: C, 60.47; H, 6.41; N, 3.71%. Found: C, 60.40; H, 6.35; N, 3.75%. Mass spectrum (LC/MS APCI): m/z 378 [$\text{M}+\text{H}$] $^+$. ^1H NMR: (CDCl_3 as solvent, δ in ppm): 1.26 (3H, t, $-\text{CH}_3$), 3.16 (2H, d, $-\text{P}-\text{CH}_2-$), 3.95 (3H, s, $-\text{OCH}_3$), 4.01 (2H, m, $-\text{CH}_2-$), 6.87–7.39 (8H, m, aromatic protons), 8.65 (1H, s, $-\text{CH}=\text{N}-$), 13.70 (H, s, $-\text{OH}$). UV-vis: (λ_{max} , nm; ϵ_{max} , $\text{M}^{-1}\text{cm}^{-1}$), CH_3OH as solvent: 430 (4.9×10^{-3}), 338 (7.3×10^{-3}), 305 (6.9×10^{-3}), 240 (8.3×10^{-4}), 225 (9.2×10^{-4}). Infrared spectrum (cm^{-1} , KBr disk): 2960, 2845 $\nu(\text{CH}_2)$, 1625 $\nu(\text{C}=\text{N})$, 1250 $\nu(\text{P}=\text{O})$.

HL^3 – Yield: 87%, m.p. 158 °C. color: orange. Analysis Calc. for $\text{C}_{18}\text{H}_{22}\text{NO}_5\text{P}$: C, 59.50; H, 6.10; N, 3.85%. Found: C, 59.47; H, 6.07; N, 3.90%. Mass spectrum (LC/MS APCI): m/z 364 [$\text{M}+\text{H}$] $^+$. ^1H NMR: (CDCl_3 as solvent, δ in ppm): 1.32 (3H, t, $-\text{CH}_3$), 3.19

Table 1
Crystallographic data of the ligands HL^1 – HL^3 .

Identification code	HL^1	HL^2	HL^3
Empirical formula	$\text{C}_{18}\text{H}_{22}\text{NO}_4\text{P}$	$\text{C}_{19}\text{H}_{24}\text{NO}_5\text{P}$	$\text{C}_{18}\text{H}_{22}\text{NO}_5\text{P}$
Formula weight	347.34	377.36	363.34
Crystal system	Triclinic	Triclinic	Monoclinic
Space group	$\text{P}\bar{1}$	$\text{P}\bar{1}$	$\text{P}2_1/\text{c}$
Unit cell a (Å)	8.8549(13)	8.6927(9)	12.588(2)
b (Å)	10.4087(15)	9.9463(11)	8.9001(16)
c (Å)	10.8325(16)	12.1329(13)	16.908(3)
α (°)	84.960(2)	78.848(2)	90
β (°)	68.491(2)	79.636(2)	105.895(3)
γ (°)	73.155(2)	66.970(2)	90
Volume (Å ³)	888.8(2)	940.85(17)	1821.9(6)
Z	2	2	4
Abs. coeff. (mm^{-1})	0.176	0.175	0.178
Refl. collected	7968	9461	17953
Ind. Refl. [R_{int}]	3626 [0.0398]	4514 [0.0254]	4517 [0.0434]
R_1, wR_2 [$I > 2(I)$]	0.0461, 0.0939	0.0435, 0.1068	0.0441, 0.1040
R_1, wR_2 (all data)	0.0780, 0.1072	0.0566, 0.1159	0.0656, 0.1161

(2H, d, $-\text{P}-\text{CH}_2-$), 4.07 (2H, m, $-\text{CH}_2-$), 6.96–7.33 (8H, m, aromatic protons), 8.41 (1H, s, $-\text{CH}=\text{N}-$). UV-vis: (λ_{max} , nm; ϵ_{max} , $\text{M}^{-1}\text{cm}^{-1}$), CH_3OH as solvent: 443 (8.4×10^{-3}), 345 (9.0×10^{-3}), 308 (3.7×10^{-3}), 246 (2.6×10^{-4}), 220 (3.2×10^{-4}). Infrared spectrum (cm^{-1} , KBr disk): 2960, 2845 $\nu(\text{CH}_2)$, 1625 $\nu(\text{C}=\text{N})$, 1250 $\nu(\text{P}=\text{O})$.

2.3. X-ray structure solution and refinement for the Schiff base ligands HL^1 – HL^3

X-ray diffraction data for these three compounds were collected at 150(2)K on a Bruker Apex II CCD diffractometer using $\text{Mo K}\alpha$ radiation ($\lambda = 0.71073$ Å). The structures were solved by direct methods and refined on F^2 using all the reflections [14]. All the non-hydrogen atoms were refined using anisotropic atomic displacement parameters and hydrogen atoms bonded to carbon were inserted at calculated positions using a riding model. Hydrogen atoms bonded to oxygen were located from difference maps and allowed to refine with temperature factors riding on those of the carrier atoms. The crystal data and details of the structure solution and refinement are given in Table 1; selected bond lengths are given in Table 2. Further experimental details have been deposited as supplementary material at the Cambridge Crystallographic Data Centre (CCDC 746866–746868).

3. Results and discussion

In this study, we obtained three novel phosphonate Schiff base compounds from the reaction of the salicylaldehyde (HL^1), 3-methoxy-2-hydroxybenzaldehyde (HL^2), 2,4-dihydroxybenzaldehyde (HL^3) and diethyl (4-aminobenzyl)phosphonate compounds in ethanol solution. Obtained compounds were characterized by the analytical and spectroscopic methods. The suitable crystals for the X-ray anal-

Table 2
Selected bond lengths(Å) of the ligands HL^1 – HL^3 .

Distance	HL^1	HL^2	HL^3
C1–O1	1.349(3)	1.3521(19)	1.352(2)
C2–O2		1.3694(19)	
C3–O3			1.355(2)
P–O	1.4655(15)	1.4699(12)	1.4754(12)
P–OR	1.5720(15)	1.5737(12)	1.5690(12)
	1.5847(15)	1.5845(12)	1.5755(12)
P–C	1.789(2)	1.7959(16)	1.7885(18)
N1–C7	1.282(3)	1.290(2)	1.284(2)
N1–C8	1.422(3)	1.4213(19)	1.421(2)

Table 3
Hydrogen bond geometry of the ligands HL¹–HL³.

	D–H...A	D–H	H...A	D...A	<(DHA)
HL ¹	O1–H1A...N1	0.88(3)	1.79(3)	2.585(2)	150(3)
HL ²	O1–H1...N1	0.88(2)	1.76(2)	2.5737(17)	153(2)
HL ³	O1–H1...N1	0.90(2)	1.74(2)	2.5824(19)	155(2)
HL ³ (intermolecular)	O2–H2...O3 ^a	0.86(2)	1.79(2)	2.6420(19)	167(2)

^a Symmetry operation $-x, 0.5+y, 0.5-z$.

ysis were obtained by recrystallization from C₂H₅OH solution. The ligands soluble in common polar organic solvents such as EtOH, MeOH, CHCl₃ and CH₂Cl₂. But, they partially soluble in apolar organic solvents such as benzene, hexane and toluene. The compounds are very stable solids at room temperature without decomposition. The ligands were obtained as coloured plate crystals in the range 72–87% yield.

In order to further information about the ligands, their ¹H NMR spectra were recorded using CDCl₃ as a solvent and spectral data were given in Section 2. The ¹H NMR spectra of the ligands were given in Supporting Information. In the spectra of the ligands, the triplets in the 1.26–1.32 ppm range can be attributed to the CH₃ hydrogen atoms. The dublets in the 3.15–3.19 ppm range may be assigned to the –P–CH₂– group protons [15]. In the spectrum of the ligand HL², the singlet at 3.95 ppm can be attributed to the –OCH₃

protons. The multiplets of the aromatic ring protons were seen in the 6.87–7.42 ppm range. The azomethine proton of the ligands were seen in the range 8.41–8.64 ppm range [16].

The electronic properties of the ligands HL¹–HL³ were investigated in the methanol solution and spectral data were given in Section 2. In the spectra of the ligands, the bands in the 443–305 nm range can be attributed to the $n-\pi^*$ transitions of the azomethine and hydroxyl groups. The bands in the 294–225 nm range may be assigned to the benzenoid $\pi-\pi^*$ transitions [17].

The infrared spectral data were given in Section 2. The bands observed in the 2960–2845 cm⁻¹ range can be attributed to the aliphatic $\nu(\text{C-H})$ vibrations. The azomethine $\nu(\text{CH=N})$ vibrations were observed in the 1625 cm⁻¹ range [18]. The $\nu(\text{P=O})$ bands of the ligands were seen in the 1245–1250 cm⁻¹ range [19].

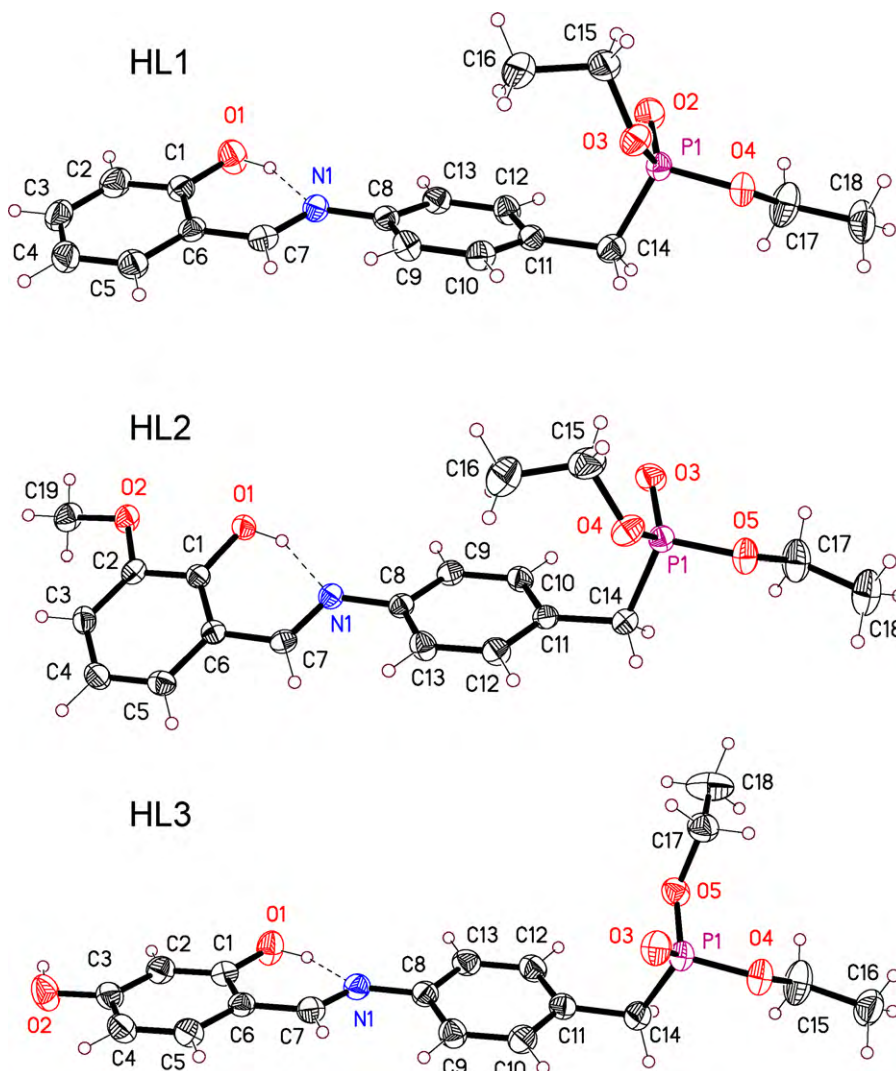


Fig. 1. ORTEP diagrams of the ligands (HL¹–HL³) with thermal ellipsoids at 50% probability.

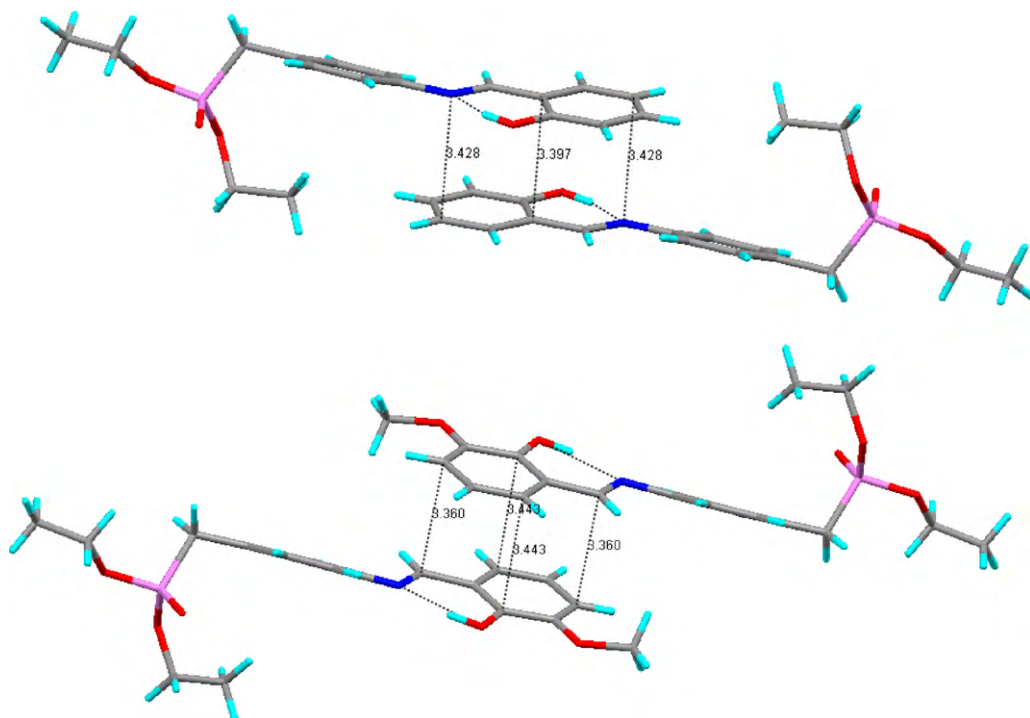


Fig. 2. Intermolecular π - π interactions in the ligands HL¹ (top) and HL² (bottom).

The mass spectral studies of the salicylidene phosphonate derivatives (HL¹ and HL³) were done and obtained data are given in Section 2. The mass spectra of the ligands were given in [Supporting Information](#). In the spectra of the ligands, the molecular ion peak [M+H]⁺ of the ligand HL³ was seen at the m/z 364. The highest intensity peak of the ligands HL¹ and HL³ were seen at m/z 303 (100%) due to the losing -OCH₂-CH₃ group. In the spectrum of the ligand HL², this peak also was seen at same region but as a very weak intensity (5%).

3.1. X-ray structure properties of the novel salicylidene phosphonate derivatives

Perspective views of all three compounds are shown in Fig. 1. All bond lengths of the compounds are in the normal ranges. The molecular structures are broadly similar, but differing principally

in the conformation about the phosphorus atom and the dihedral angle between the two aromatic rings.

Selected bond lengths (Å) of the ligands HL¹-HL³ were given in Table 2. Three ligands have also intramolecular phenol-imine hydrogen bonds between the atoms O1-N1 (Table 3). The ligand HL³ contains a second phenol group and this group makes an intermolecular hydrogen bond with the phosphine oxide group of a neighbouring molecule O2-O3 (under symmetry operation $-x, 0.5 + y, 0.5 - z$), linking the molecules into H-bonded chains (Fig. 1). There are no similar interactions in the compounds HL¹ and HL². In addition, these ligands show distinct the π - π interactions.

The dihedral angles between the two aromatic rings are 16.93(10), 24.40(8) and 8.48(12) $^\circ$, for HL¹, HL² and HL³, respectively. This difference reflects the different intermolecular interactions in the lattice. There is a evidence of π - π phenyl stacking in both HL¹ and HL². In the ligand HL¹, the phenol-imine

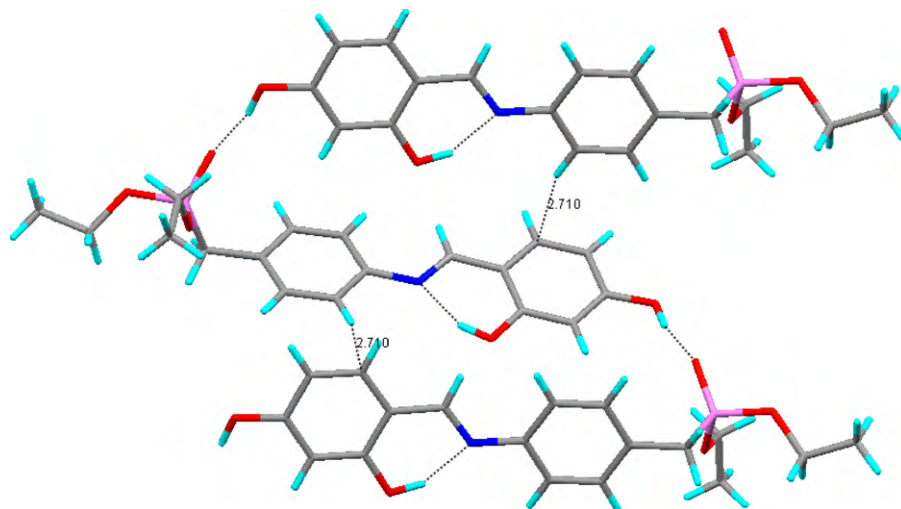


Fig. 3. H-bonding and C-H- π interactions in the ligand HL³.

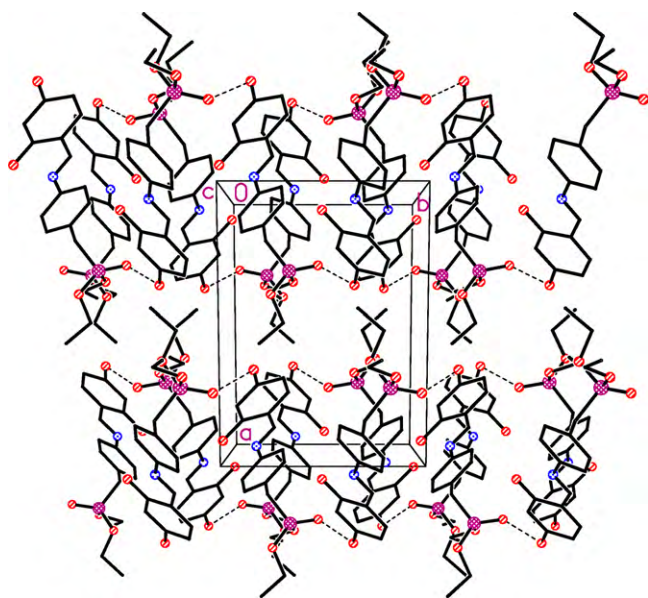


Fig. 4. Unit cell packing for HL³.

fragment of the ligand (C1–N1) is stacked with the same section of an adjacent molecule having symmetry operation $2-x, 1-y, -z$ with interplanar separation with 3.40 Å. The C6 numbered carbon atoms of the ligands HL¹ and HL² are separated by with 3.397 Å (Fig. 2). There is similar stacking in compound HL² under symmetry operation $2-x, 1-y, -z$ with interplanar separation of 3.40 Å. The C3 and C7 carbon atoms are separated by 3.360 Å. The distance between two adjacent phenyl rings of the ligand HL¹ is longer according to the ligand HL². There is no evidence of π – π stacking in HL³. Presumably, it is not compatible with the intermolecular hydrogen bond, however, there are some edge-to-face C–H... π interactions (Fig. 3). The different intermolecular interactions between the ligands are reflected in the unit cell packing of the three molecules. Unit cell plots of the ligands HL¹ and HL² show π – π stacking dominates (Fig. 4). Whereas, the most striking feature of the ligand HL³ is the formation of H-bonded chains running parallel to *b* (Fig. 5).

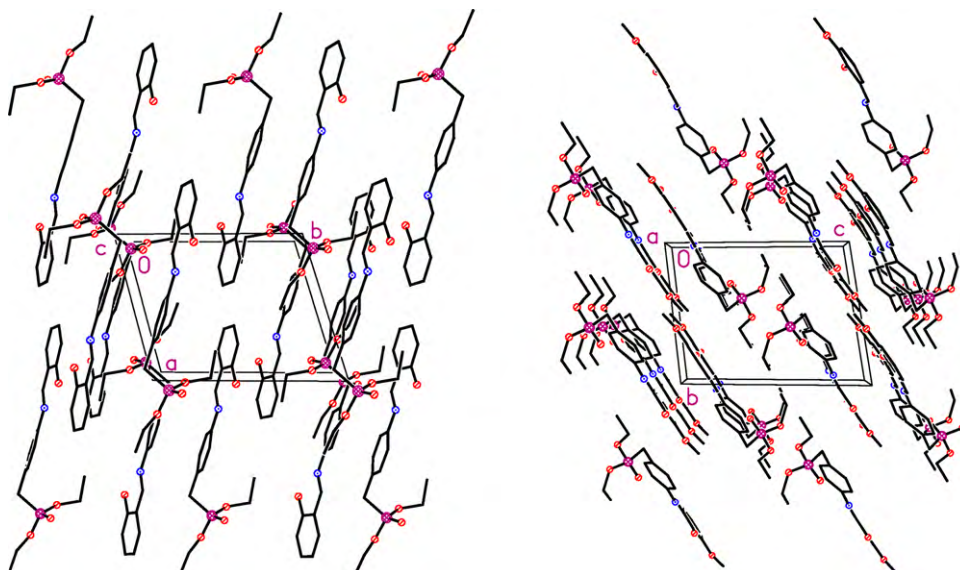


Fig. 5. Packing diagrams for HL¹ and HL².

3.2. Electrochemical properties of the ligands

Electrochemical studies of the novel salicylidene phosphonate derivatives (HL¹–HL³) were run in CH₃CN/C₂H₅OH (v/v, 1:1) mixture at 293 K. The studies were done both reduction and oxidation at pH 2–12 in Britton–Robinson buffer and in the (+2000) – (–2000) potential range. When the peak current–pH relationship was investigated, the highest peak current value was obtained at pH 3. HL¹–HL³ appear to be an electroactive compound for both directions. Specifically, the compounds are capable to be both oxidable and reducible. To demonstrate the usefulness of a solid electrode for investigation of HL¹–HL³, which may offer advantages for the use of such electrodes as sensors, the electrochemical behaviour of HL¹–HL³ on a glassy carbon electrode was investigated in this research. Therefore, several measurements with different electrochemical parameters were performed using various supporting electrolytes (0.1 M H₂SO₄, 0.5 M H₂SO₄, 0.2 M phosphate buffer at pH 2.0–9.0, 0.04 M Britton–Robinson buffer at pH 2.32–12.0 and 0.2 M acetate buffer at pH 3.5–5.5) and buffers in order to obtain such information. Cyclic voltammograms of HL¹–HL³ exhibited one distinct and well-defined cathodic peak at ~ -0.5 V and ill-defined anodic wave at $\sim +0.5$ at pH 3.0. The effects of potential scan rates (ν) between 5 and 1000 mV s^{–1} on the peak potential and peak current of compounds were also evaluated. Scan rate studies were then carried out to assess whether the processes on glassy carbon electrode were under diffusion or adsorption control. A linear relationship on the oxidation peak current (I_p) with the square root of the scan rate ($\nu^{1/2}$) showed the diffusion control process. The equation is noted below in Britton–Robinson buffer at pH 3:

$$I_p (\mu\text{A}) = 0.221 \nu^{1/2} (\text{mV s}^{-1}) + 2.089$$

$$(r = 0.991, n = 10 \text{ for starting material})$$

$$I_p (\mu\text{A}) = 0.363 \nu^{1/2} (\text{mV s}^{-1}) + 0.021 \quad (r = 0.990, n = 10, \text{ for HL}^1)$$

$$I_p (\mu\text{A}) = 0.478 \nu^{1/2} (\text{mV s}^{-1}) + 2.956 \quad (r = 0.991, n = 10, \text{ for HL}^2)$$

$$I_p (\mu\text{A}) = 0.981 \nu^{1/2} (\text{mV s}^{-1}) + 0.603 \quad (r = 0.991, n = 10, \text{ for HL}^3)$$

The effect of scan rate on peak current was also examined under the above conditions with a plot of logarithm of peak current ($\log i$)

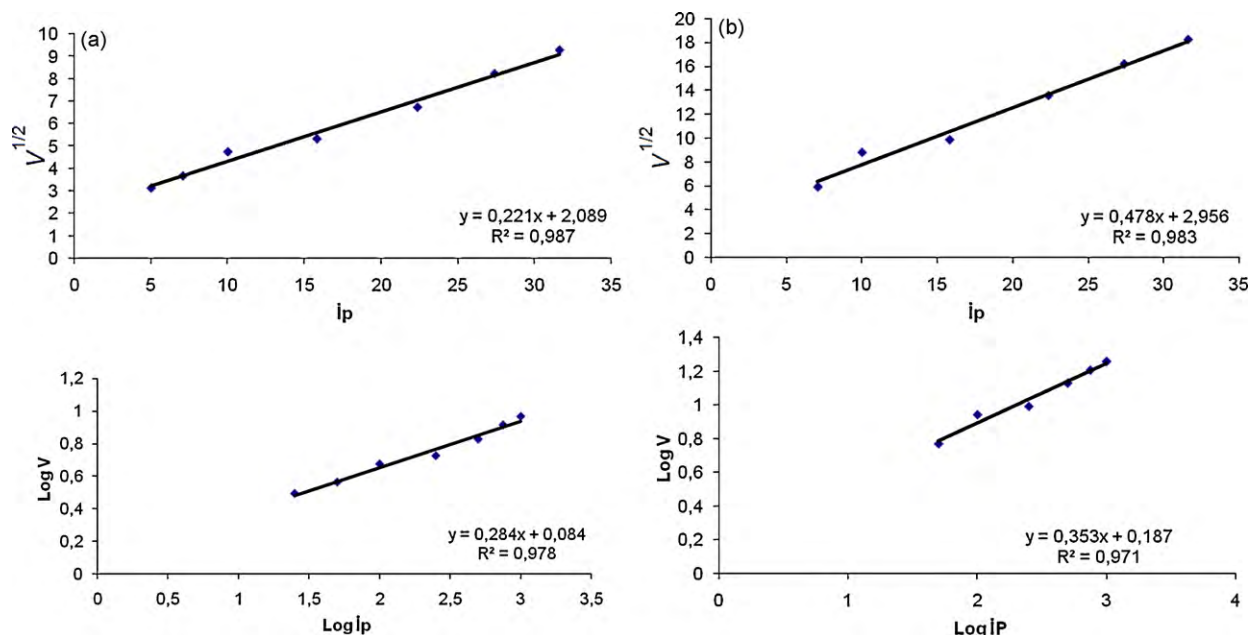


Fig. 6. (a) Typical $I_p-v^{1/2}$ and $\log ip-\log v$ curves for starting material. (b) Typical $I_p-v^{1/2}$ and $\log ip-\log v$ curves for HL^2 .

versus logarithm of scan rate ($\log v$), giving a straight line within the same scan rate range. This linear relationship was obtained as follow:

$$\log ip (\mu A) = 0.284 \log v (mV s^{-1}) + 0.084$$

($r = 0.991$, $n = 10$ for starting material)

$$\log ip (\mu A) = 0.174 \log v (mV s^{-1}) + 0.061 \quad (r = 0.995, n = 10 \text{ for } HL^1)$$

$$\log ip (\mu A) = 0.353 \log v (mV s^{-1}) + 0.187 \quad (r = 0.985, n = 10 \text{ for } HL^2)$$

$$\log ip (\mu A) = 0.459 \log v (mV s^{-1}) + 0.109 \quad (r = 0.985, n = 10 \text{ for } HL^3)$$

The slopes (between 0.174 and 0.459) of the relationship are close to the theoretically expected (0.5) for an ideal reaction of solution species [20,21], so in this case the process had a diffusive component. Typical $I_p-v^{1/2}$ and $\log ip-\log v$ curves and cyclic voltammograms of 1×10^{-4} M starting material and HL^2 have been given in Figs. 6 and 7 Fig. 6a and b and Fig. 7, respectively.

4. Supplementary material

Crystallographic data for structural analysis has been deposited with the Cambridge Crystallographic Data Centre, CCDC 746866–746868 for the reported ligands (HL^1 – HL^3). Copies of this information may be obtained free of charge from The Director, CCDC, 12 Union Road, Cambridge, CB2 1EZ, UK (fax: +44 1223 336033; deposit@ccdc.cam.ac.uk or www.ccdc.cam.ac.uk).

Appendix A. Supplementary data

Supplementary data associated with this article can be found, in the online version, at doi:10.1016/j.saa.2010.05.011.

References

- [1] H. Schiff, Ann. Suppl. 3 (1864) 343–370.
- [2] E.J. Larson, V.L. Pecoraro, J. Am. Chem. Soc. 113 (1991) 3810–3818.
- [3] A. Mukherjee, R. Raghunathan, M.K. Saha, M. Nethaji, S. Ramasesha, A.R. Chakravarty, Chem. Eur. J. 11 (2005) 3087–3096.
- [4] J. Chakraborty, R.N. Patel, J. Indian Chem. Soc. 73 (1996) 191–193.
- [5] R. Klement, F. Stock, H. Elias, H. Paulus, P. Pelikan, M. Valko, M. Mazur, Polyhedron 18 (1999) 3617–3628.
- [6] F. Marchetti, C. Pettinari, R. Pettinari, A. Cingolani, D. Leanesi, A. Lorenotti, Polyhedron 18 (1999) 3041–3050.
- [7] C.G. Zhang, J. Sun, X.F. Kong, C.X. Zhao, J. Coord. Chem. 50 (2000) 353–362.
- [8] P.G. Ramappa, J. Indian Chem. Soc. 76 (1999) 235–238.

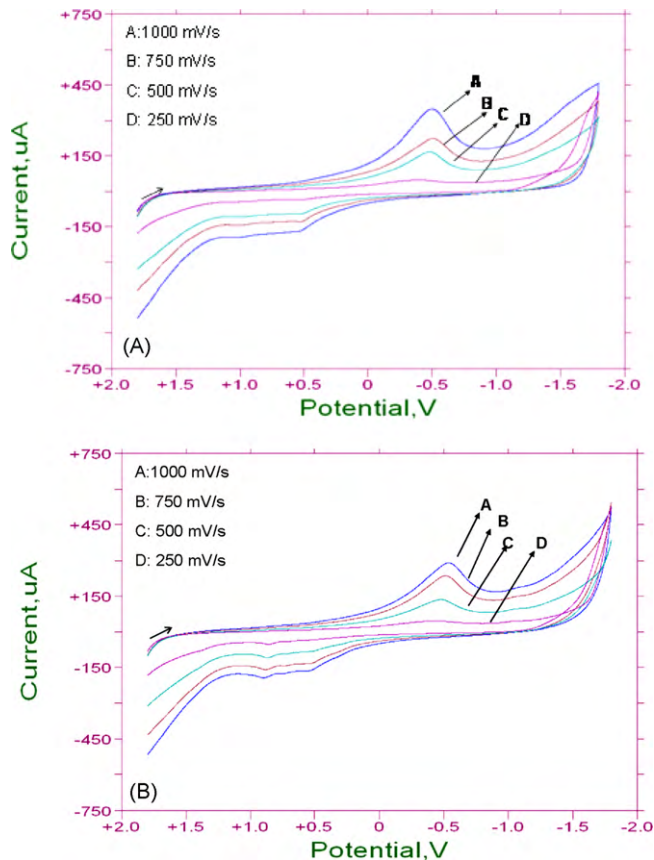


Fig. 7. Cyclic voltammograms of 1×10^{-4} M starting material (A) and HL^2 (B).

- [9] P.L. Gurian, L.K. Cheatham, J.W. Ziller, A.R. Barron, *J. Chem. Soc. Dalton Trans.* (1991) 1449–1456.
- [10] E. Labisbal, J.A. Garcia-Vazquez, J. Romero, S. Picos, A. Sousa, *Polyhedron* 14 (1995) 663–670.
- [11] A.A. Soliman, W. Linert, *Thermochim. Acta* 338 (1999) 67–75.
- [12] N. Mondal, S. Mitra, V. Gramlich, S.O. Ghodsi, K.M.A. Malik, *Polyhedron* 20 (1999) 135–141.
- [13] H. Sigel, S.S. Massoud, N.A. Corfu, *J. Am. Chem. Soc.* 116 (1944) 2958–2971.
- [14] G.M. Sheldrick, *Acta Cryst. A* 64 (2008) 112–122.
- [15] C.A. Tellez, S.V. de Souza, W.O. Lin, *Spectrochim. Acta A* 56 (2000) 653–669.
- [16] M. Dolaz, V. McKee, A. Gölcü, M. Tümer, *Curr. Org. Chem.* 14 (2010) 281–288.
- [17] M. Tümer, *Synth. React. Inorg. Met. Org. Chem.* 30 (2000) 1139–1158.
- [18] M. Tümer, *J. Coord. Chem.* 60 (2007) 2051–2065.
- [19] E.E. İltter, Z. Kılıç, *Spectrochim. Acta A* 70 (2008) 542–549.
- [20] A. Golcu, B. Dogan, S.A. Ozkan, *Talanta* 67 (2005) 703–712.
- [21] E. Laviron, *J. Electroanal. Chem.* 112 (1980) 11–23.